
**MAGNETISM
AND FERROELECTRICITY**

Magnetic Properties of Copper Metaborate: Two-Parameter Phenomenological Model

M. A. Popov*, G. A. Petrakovskii, and V. I. Zinenko****

* *Krasnoyarsk State University, Krasnoyarsk, 660041 Russia*

** *Kirensky Institute of Physics, Siberian Division, Russian Academy of Sciences,
Akademgorodok, Krasnoyarsk, 660036 Russia*

e-mail: rsa@iph.krasn.ru

Received July 21, 2003

Abstract—Symmetry analysis is performed for the magnetic subsystem of copper metaborate, and a phenomenological model is proposed with two two-component order parameters that correspond to ferromagnetism and antiferromagnetism vectors lying in the tetragonal plane of this crystal. Owing to the $I\bar{4}2d$ space group of symmetry of this crystal, the thermodynamic potential contains the Lifshitz invariant having the form of an anti-symmetric product of the order parameters and their spatial derivatives. Analysis of this model shows that the temperatures of ordering in the magnetic subsystem and of the formation of a spiral structure in it can be different. This fact allows numerical calculation of the temperature dependences of the spiral wave vector, magnetization, and intensities of first- and third-order magnetic satellites in the incommensurate phase that arise in neutron elastic scattering, as well as the field dependence of the magnetization. The experimental data, including a magnetic-field-temperature phase diagram, are satisfactorily described. The parameters of the phenomenological thermodynamic potential of the magnetic subsystem of copper metaborate are estimated. © 2004 MAIK “Nauka/Interperiodica”.

1. INTRODUCTION

Copper oxide compounds exhibit a wide variety of types of magnetic ordering and magnetic properties. Such compounds include not only various collinear ferromagnets but also weak ferromagnets, spin glasses, singlet magnets, ferrimagnets, and incommensurate magnetic structures. Interest in the magnetic properties of these materials has quickened due to the discovery of high-temperature superconductors, in which magnetic correlations are likely to play an important role in the formation of a superconducting state.

As shown in [1–5], copper metaborate CuB_2O_4 has especially interesting magnetic properties. According to the neutron diffraction data and magnetic measurements, the magnetic subsystem of this crystal transforms from a paramagnetic state into an easy-plane weak ferromagnet at $T_N = 20$ K. However, the temperature dependences of the specific heat and magnetic susceptibility in the tetragonal plane of the crystal exhibit specific features not only at T_N but also at $T_i = 10$ K. The magnetic peaks observed in neutron diffraction patterns in the temperature range from T_N to T_i coincide with the lattice peaks, which reflects the coincidence of the magnetic unit cell and the crystal unit cell [3]. Therefore, the phase transition at T_N corresponds to a wave vector at the center of the Brillouin zone, $\mathbf{q} = 0$.

The special high-resolution neutron diffraction study reported in [3] showed that the crystal did not undergo any structural phase transitions down to a tem-

perature of 1.5 K. However, as the temperature decreases below T_i , magnetic satellites appear in the neutron diffraction patterns in symmetrical positions with respect to the reciprocal-lattice points of the commensurate phase. These satellites were attributed to a periodic magnetic structure that is incommensurate to the lattice structure along the tetragonal axis of the crystal and represents a spin-density phase-modulated wave [3]. The presence of higher order magnetic satellites generated by the incommensurate phase in neutron diffraction patterns near T_i indicates the formation of a magnetic soliton lattice.

Studies of elastic neutron scattering in strong magnetic fields have shown that the incommensurate magnetic structure in copper metaborate undergoes a first-order transition into a commensurate phase when the magnetic field reaches a certain critical value that is dependent on temperature [4, 5].

To the best of our knowledge, there is only one case (described in [6] for the NiBr_2 crystal) where the transition from a commensurate to an incommensurate phase also occurs with decreasing temperature. Since the symmetry of NiBr_2 prohibits any Lifshitz invariants, the mechanism of the appearance of the incommensurate phase in the crystal is related to a possible temperature dependence of competing exchange interactions [6]. As will be shown below, the symmetry of copper metaborate allows a small relativistic Lifshitz invariant having an unconventional form. This invariant

allows one to phenomenologically describe the unusual sequence of phase transitions observed in copper metaborate and a number of its magnetic properties.

2. INCOMPLETE THERMODYNAMIC POTENTIAL OF COPPER METABORATE

The x-ray diffraction and neutron diffraction studies performed in [3] at room temperature showed that copper metaborate belongs to the space group $I\bar{4}2d$ and its lattice parameters are $a = 11.528 \text{ \AA}$ and $c = 5.607 \text{ \AA}$. The unit cell contains twelve formula units. The Cu^{2+} ions occupy two nonequivalent positions; namely, $\text{Cu}(b)$ is in the $4b$ position with point symmetry S_4 (0,0,1/2) and $\text{Cu}(d)$ is in the $8d$ position with point symmetry C_2 (0.0815, 1/4, 1/8). The $\text{Cu}(b)$ ion is at the center of the square formed by four oxygen ions, and the $\text{Cu}(d)$ ion is surrounded by six oxygen ions localized at the vertices of a distorted octahedron.

The point group $\bar{4}2m$ of the crystal contains eight symmetry elements [7]:

$$1, \bar{4}_3^-, 4_3^2, \bar{4}_3^3, 4_1^2, 4_2^2, m_4, m_5.$$

This group has five irreducible representations. Four of them ($\Gamma_1, \Gamma_2, \Gamma_3, \Gamma_4$) are one-dimensional, and one (Γ_5) is two-dimensional. The reductions of the magnetic representations for the two nonequivalent copper sublattices in copper metaborate have the form

$$\Gamma_{4b} = \Gamma_1 + \Gamma_2 + 2\Gamma_5,$$

$$\Gamma_{8d} = \Gamma_1 + 2\Gamma_2 + 2\Gamma_3 + \Gamma_4 + 3\Gamma_5.$$

The magnetic modes that transform according to irreducible representations of the group $\bar{4}2m$ in the $\text{Cu}(b)$ copper ion sublattice are

$$\Gamma_1: S_{b1z} - S_{b2z},$$

$$\Gamma_2: S_{b1z} + S_{b2z},$$

$$\Gamma_5: (S_{b1x} + S_{b2x}, -S_{b1y} - S_{b2y}), \quad (1)$$

$$\Gamma_5: (S_{b1y} - S_{b2y}, S_{b1x} - S_{b2x}). \quad (2)$$

The modes corresponding to the representations Γ_1 and Γ_2 of the $4b$ position describe antiferromagnetic and ferromagnetic ordering along the tetragonal c axis, respectively, while the modes related to the representation Γ_5 describe a noncollinear magnetic structure in the tetragonal plane. For the $\text{Cu}(d)$ copper ion sublattice, the magnetic modes transform as follows:

$$\Gamma_1: S_{d1x} + S_{d2y} - S_{d3x} - S_{d4y},$$

$$\Gamma_2: S_{d1y} - S_{d2x} - S_{d3y} + S_{d4x},$$

$$\Gamma_2: S_{d1z} + S_{d2z} + S_{d3z} + S_{d4z},$$

$$\Gamma_3: S_{d1y} + S_{d2x} - S_{d3y} - S_{d4x},$$

$$\Gamma_3: S_{d1z} - S_{d2z} + S_{d3z} - S_{d4z},$$

$$\Gamma_4: S_{d1x} - S_{d2y} - S_{d3x} + S_{d4y},$$

$$\Gamma_5: (S_{d1x} + S_{d2x} + S_{d3x} + S_{d4x}, \quad (3)$$

$$-S_{d1y} - S_{d2y} - S_{d3y} - S_{d4y}),$$

$$\Gamma_5: (S_{d1x} - S_{d2x} + S_{d3x} - S_{d4x}, \quad (4)$$

$$S_{d1y} - S_{d2y} + S_{d3y} - S_{d4y}),$$

$$\Gamma_5: (S_{d2z} - S_{d4z}, S_{d1z} - S_{d3z}).$$

The numeration of ions for this sublattice corresponds to the sequential application of the $\bar{4}_3^1$ symmetry operation.

An incommensurate inhomogeneous phase should be described by inhomogeneous magnetic modes. The modes that are linear in the spatial derivative along the c axis are

$$\Gamma_3: (S_{b1z} - S_{b2z})',$$

$$\Gamma_4: (S_{b1z} + S_{b2z})',$$

$$\Gamma_5: (-S_{b1y} - S_{b2y}, S_{b1x} + S_{b2x})',$$

$$\Gamma_5: (S_{b1x} - S_{b2x}, S_{b1y} - S_{b2y})',$$

for the $4b$ position and

$$\Gamma_1: (S_{d1y} + S_{d2x} - S_{d3y} - S_{d4x})',$$

$$\Gamma_1: (S_{d1z} - S_{d2z} + S_{d3z} - S_{d4z})',$$

$$\Gamma_2: (S_{d1x} - S_{d2y} - S_{d3x} + S_{d4y})',$$

$$\Gamma_3: (S_{d1x} + S_{d2y} - S_{d3x} - S_{d4y})',$$

$$\Gamma_4: (S_{d1y} - S_{d2x} - S_{d3y} + S_{d4x})',$$

$$\Gamma_4: (S_{d1z} + S_{d2z} + S_{d3z} + S_{d4z})',$$

$$\Gamma_5: (-S_{d1y} - S_{d2y} - S_{d3y} - S_{d4y},$$

$$S_{d1x} + S_{d2x} + S_{d3x} + S_{d4x})',$$

$$\Gamma_5: (S_{d1y} - S_{d2y} + S_{d3y} - S_{d4y},$$

$$S_{d1x} - S_{d2x} + S_{d3x} - S_{d4x})',$$

$$\Gamma_5: (S_{d1z} - S_{d3z}, S_{d2z} - S_{d4z})',$$

for the $8d$ position, where $f' \equiv df/dz$.

Analysis of the neutron diffraction pattern [3] consisting of 25 purely magnetic peaks showed that the spins of both the $\text{Cu}(b)$ and $\text{Cu}(d)$ sublattices of copper metaborate form a noncollinear magnetic structure in the commensurate phase ($T_i < T < T_N$). In the $\text{Cu}(b)$ sublattice, the antiferromagnetism vector in the tetragonal plane is dominant, while the ferromagnetism vector

that is perpendicular to this vector and also lies in the tetragonal plane, as well as the antiferromagnetism vector along the c axis, is relatively small. In the $\text{Cu}(d)$ sublattice, the antiferromagnetism vector along the c axis is likely to be dominant, while the orthogonal antiferromagnetism vector in the tetragonal plane is relatively small. A ferromagnetism vector in this sublattice has not been detected within the limits of experimental error. In the commensurate phase, the magnetic moment of a copper ion in the $8d$ position is far less than that of a copper ion in the $4b$ position. All vectors indicated above correspond to the magnetic modes found in the symmetry analysis.

In the incommensurate phase ($T < T_i$), the magnetic structure is ordered in the tetragonal plane in the form of a spiral along the c axis. For theoretical analysis of the magnetic properties of copper metaborate in terms of the phenomenological thermodynamic potential, it is essential that its symmetry group not contain inversion center $\bar{1}$. This operation enters only in combination with 90° rotation about the c axis, namely, $\bar{4}_3^1$ and $\bar{4}_3^3$. Therefore, the thermodynamic potential can contain a Lifshitz-type invariant that should be bilinear in the two-component order parameters and their spatial derivatives and be responsible for the appearance of an incommensurate phase.

Taking into account all eight single-component and five two-component homogeneous magnetic modes in the framework of the phenomenological approach results in an extremely cumbersome expression for the thermodynamic potential of the system. Therefore, it is necessary to separate modes that allow one to describe the basic experimental properties of copper metaborate. Since ordering in the tetragonal plane is dominant, we first consider the corresponding two-component modes. The following circumstance should be taken into account in this case. If we represent an arbitrary i th homogeneous mode in the Γ_5 representation in the form $\eta_i = (\eta_{i1}, \eta_{i2})$, then the corresponding inhomogeneous mode in this representation is $\eta_i' = (\eta_{i2}, \eta_{i1})'$. The invariant $\eta_i \cdot \eta_i' = \eta_{i1}\eta_{i2}' + \eta_{i1}'\eta_{i2}$ turns out to be the complete derivative with respect to z , and it is impossible to construct a Lifshitz invariant for a single mode. In terms of the theory of representations, this feature is due to the fact that the antisymmetric square $\{\Gamma_5^2\}$ transforms according to the representation Γ_2 , the vector component parallel to the tetragonal axis transforms according to the representation Γ_3 , and the perpendicular component transforms according to the representation Γ_5 [8].

Let us represent the incomplete thermodynamic potential as a functional of two two-component order parameters, $\eta_1 = (\eta_{11}, \eta_{12})$ and $\eta_2 = (\eta_{21}, \eta_{22})$:

$$\begin{aligned} \Phi\{\eta\} = \int & \left\{ \frac{A_{11}}{2} \eta_1 \cdot \eta_1 + \frac{A_{22}}{2} \eta_2 \cdot \eta_2 + A_{12} \eta_1 \cdot \eta_2 \right. \\ & + \frac{B_{22}}{4} (\eta_2 \cdot \eta_2)^2 + C_{12} (\eta_1 \cdot \eta_2' - \eta_1' \cdot \eta_2) \\ & \left. + \frac{D_{11}}{2} \nabla \eta_1 \cdot \nabla \eta_1 \right. \end{aligned} \quad (5)$$

$$\left. + \frac{D_{22}}{2} \nabla \eta_2 \cdot \nabla \eta_2 + D_{12} \nabla \eta_1 \cdot \nabla \eta_2 - \eta_1 \cdot H_1 \right\} dV,$$

where integration is performed over the entire volume of the crystal, $A_{11} = a_{11}(T - T_1)$, $A_{22} = a_{22}(T - T_2)$, $a_{11} > 0$, $a_{22} > 0$, $B_{22} > 0$, $D_{11} > 0$, $D_{11}D_{22} > D_{12}^2$, $\nabla \eta_\alpha = (\nabla \eta_{\alpha 2}, \nabla \eta_{\alpha 1})$, and H_1 is the field conjugate to the parameter η_1 . The order parameters are assumed to be dependent on spatial coordinates.

The parameters η_1 and η_2 are different linear combinations of the magnetic modes transforming according to the representation Γ_5 . The fact that the magnetic subsystem of copper metaborate below T_N is an easy-plane weak ferromagnet spiraling below T_i allows one to compose the parameter η_1 from ferromagnetic modes described by Eqs. (1) and (3) and the parameter η_2 from antiferromagnetic modes given by Eqs. (2) and (4). Correspondingly, $H_1 = (H_{11}, H_{12}) = (H_x, -H_y)$. However, a weak ferromagnet is characterized by $T_1 \approx 0$ and $T_2 \approx T_N$. It should be noted that, unlike in [3], the order parameter responsible for the transition at T_i is not chosen in an explicit form in the thermodynamic potential (5).

The invariant with coefficient C_{12} is the known Lifshitz invariant [8] generalized to the case of two two-component order parameters; namely, this invariant is the antisymmetric product of different order parameters and their spatial derivatives rather than the antisymmetric product of the components of a single order parameter and their spatial derivatives.

Out of the invariants of the fourth order, only the invariant related to the temperature dependence of the antiferromagnetic parameter is retained in Eq. (5). The invariants that are quadratic in the spatial derivatives of the order parameters are taken in the simplest isotropic form. The presence of the other order parameters in Eq. (5), as will be shown below, is not a decisive factor for describing the evolution of the structure of copper metaborate with decreasing temperature from the paramagnetic phase above 20 K to the incommensurate phase below 10 K.

3. EQUILIBRIUM STATE IN THE MODEL

In the absence of the Lifshitz invariant, the equilibrium state in the model described by phenomenological potential (5) is homogeneous because of the positive definiteness of the other inhomogeneous terms of the potential. The Lifshitz invariant disturbs the stability of this state along the tetragonal axis. To find a new equilibrium state, we use the fact that higher order magnetic satellites in neutron diffraction patterns in the absence of an applied dc magnetic field were detected only in the vicinity of the transition to the incommensurate phase [2, 3].

Therefore, we represent the equilibrium state in a zero applied field in the form

$$\begin{aligned} \eta_1 &= (p_{11} \cos(qz + \phi_{11}), p_{12} \cos(qz + \phi_{12})), \\ \eta_2 &= (p_{21} \cos(qz + \phi_{21}), p_{22} \cos(qz + \phi_{22})), \end{aligned} \tag{6}$$

where the amplitudes $p_{\alpha\beta}$ and the phases $\phi_{\alpha\beta}$ of a spatial wave are independent of z . Putting $\phi_{11} = 0$ in Eq. (6), we set a reference point along the tetragonal axis without loss of generality. The set of necessary conditions for an extremum that is obtained from Eq. (5) by variation with respect to the parameters given in Eq. (6) is rather awkward. We give only its solution:

$$\begin{aligned} p_{11} &= -(A_{12q}p_{21} - C_{12q}p_{22})/A_{11q}, \\ p_{12} &= -(A_{12q}p_{21} + C_{12q}p_{22})/A_{11q}, \end{aligned} \tag{7}$$

$$\begin{aligned} p_{21} &= p_{22} \\ &= \text{Re}\{[(A_{12q}^2 + C_{12q}^2 - A_{11q}A_{22q})/A_{11q}B_{22}]^{1/2}\}, \end{aligned} \tag{8}$$

$$q = \text{Re}\left\{\left[\frac{\left(\frac{4A_{11}D_{11}C_{12}^2 - (A_{11}D_{12} - A_{12}D_{11})^2}{D_{11}D_{22} - D_{12}^2}\right)^{1/2} - A_{11}}{D_{11}}\right]^{1/2}\right\}, \tag{9}$$

$$\phi_{11} = \phi_{21} = 0, \quad \phi_{12} = \phi_{22} = \pi/2, \tag{10}$$

where $A_{\alpha\beta q} = A_{\alpha\beta} + D_{\alpha\beta}q^2$ and $C_{12q} = 2C_{12}q$.

Unlike the relationships in [9] considered for a one-parameter potential, these relationships feature a possible difference between the temperature of ordering in the magnetic system ($p_{21} \neq 0$) and the temperature of formation of a spiral structure in it ($q \neq 0$). For example, a spiral magnetic structure exists in the temperature range (T_{q1}, T_{q2}) with

$$T_{q1} = T_{q0} - \Delta T_q, \quad T_{q2} = T_{q0} + \Delta T_q, \tag{11}$$

where

$$T_{q0} = T_1 + (A_{12}D_{12} + 2C_{12}^2)/(a_{11}D_{22}),$$

$$\Delta T_q = [(A_{12}D_{12} + 2C_{12}^2)^2 - A_{12}^2D_{11}D_{22}]^{1/2}/(a_{11}D_{22}).$$

Ordering occurs at the temperature

$$T_p = T_{p0} + \Delta T_p,$$

$$T_{p0} = [T_1 + T_2 - (D_{11}/a_{11} + D_{22}/a_{22})q^2]/2, \tag{12}$$

$$\begin{aligned} \Delta T_p &= \{[T_1 - T_2 - (D_{11}/a_{11} - D_{22}/a_{22})q^2]^2 \\ &\quad + 4(A_{12q}^2 + C_{12q}^2)/(a_{11}a_{22})\}^{1/2}/2. \end{aligned}$$

Note that, in the incommensurate phase, according to Eqs. (7), (8), and (10), the order parameter η_1 forms an elliptical spiral along the tetragonal axis and the order parameter η_2 , a circular spiral. The ellipticity of the spiral means that the magnetic moments deviate from the

tetragonal plane to form a wave of their components that are parallel to the tetragonal axis.

We describe the state of the crystal in an external magnetic field applied along the tetragonal plane with the equations

$$\begin{aligned} \eta_1 &= (p_{11q} \cos(qz + \phi_{11q}) + p_{11k} \cos(kz + \phi_{11k}), \\ &\quad p_{12q} \cos(qz + \phi_{12q}) + p_{12k} \cos(kz + \phi_{12k})), \end{aligned} \tag{13}$$

$$\begin{aligned} \eta_2 &= (p_{21q} \cos(qz + \phi_{21q}) + p_{21k} \cos(kz + \phi_{21k}), \\ &\quad p_{22q} \cos(qz + \phi_{22q}) + p_{22k} \cos(kz + \phi_{22k})), \end{aligned}$$

$$H_1 = (H \cos(kz), -H \sin(kz)).$$

The passage to the case of a homogeneous applied field ($k = +0$) in $\Phi\{\eta\}$ should be performed only after integrating over the volume of the crystal.

The variational equations permit two solutions characterized by the following common relations:

$$\begin{aligned} p_{11q} &= -(A_{12q}p_{21q} - C_{12q}p_{22q})/A_{11q}, \\ p_{12q} &= -(A_{12q}p_{21q} + C_{12q}p_{22q})/A_{11q}, \\ p_{11k} &= (H - A_{12}p_{21k})/A_{11}, \\ p_{12k} &= (H - A_{12}p_{22k})/A_{11}, \end{aligned} \tag{14}$$

$$\begin{aligned} \phi_{11q} &= \phi_{21q} = \phi_{11k} = \phi_{21k} = 0, \\ \phi_{12q} &= \phi_{22q} = \phi_{12k} = \phi_{22k} = \pi/2. \end{aligned}$$

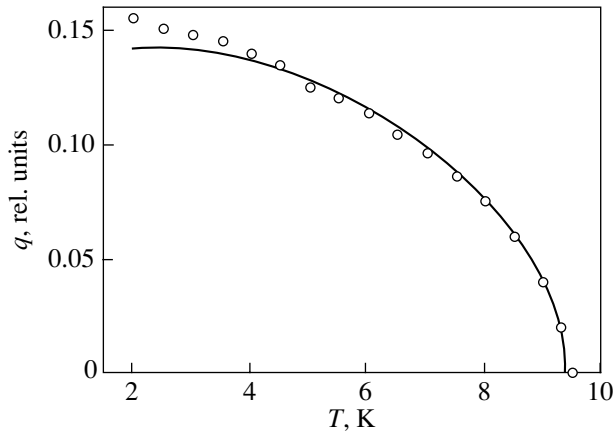


Fig. 1. Temperature dependence of the wave vector of the magnetic structure in copper metaborate at a zero applied field. Points are experimental data and the solid line is calculation.

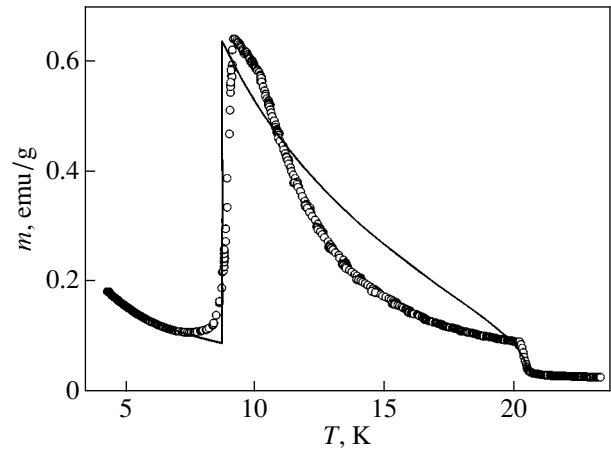


Fig. 2. Temperature dependence of the magnetization of single-crystalline copper metaborate in an applied field of 0.25 kOe in the tetragonal plane.

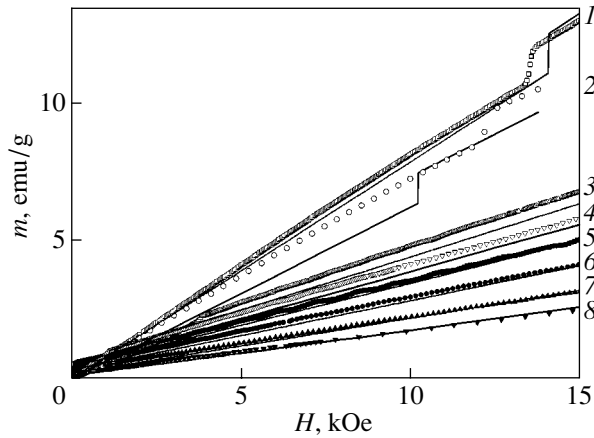


Fig. 3. Field dependence of the magnetization of single-crystalline copper metaborate in the tetragonal plane at various temperatures: (1) $T = 4.2$, (2) 5, (3) 8, (4) 9, (5) 10, (6) 12, (7) 15, and (8) 18 K.

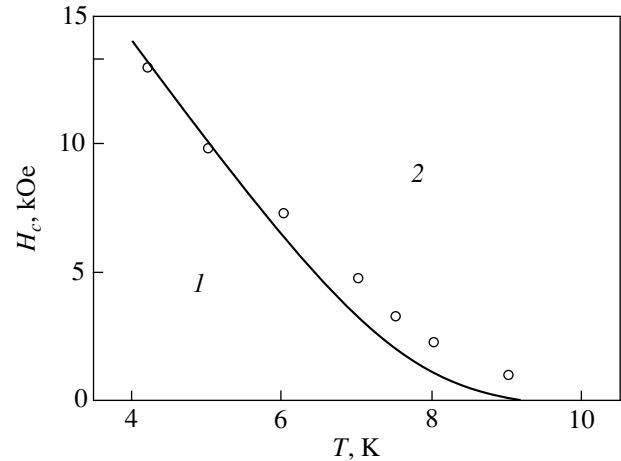


Fig. 4. Temperature–field phase diagram of copper metaborate: (1) incommensurate phase and (2) easy-plane weak-ferromagnetic phase.

One solution corresponds to a homogeneous state of the magnetic system,

$$p_{21q} = p_{22q} = 0, \quad p_{21k} = p_{22k} = p_{2k}, \quad (15)$$

where p_{2k} satisfies the equation

$$A_{11}B_{22}p_{2k}^3 + (A_{11}A_{22} - A_{12}^2)p_{2k} + A_{12}H = 0.$$

The other solution describes an inhomogeneous state,

$$p_{21q} = p_{22q} = p_{2q}, \quad p_{21k} = p_{22k} = p_{2k}, \quad (16)$$

where p_{2q} and p_{2k} are determined from the set of equations

$$A_{11q}B_{22}p_{2q}^2 + A_{11q}(A_{22q} + 2B_{22}p_{2k}^2) = A_{12q}^2 + C_{12q}^2,$$

$$3A_{11}A_{11q}B_{22}p_{2k}^3 + [2A_{11}A_{11q}A_{22q} + A_{11q}A_{12}^2 - A_{11}A_{11q}A_{22} - 2A_{11}(A_{12q}^2 + C_{12q}^2)]p_{2k} = A_{11q}A_{12}H.$$

The wave vector \mathbf{q} is equal to zero or determined by Eq. (9) depending on the stability of the corresponding solutions (15) or (16). The stability of a solution depends on the relation between the parameters of thermodynamic potential (5) and the value of the magnetic field.

4. DISCUSSION OF THE RESULTS

The case where the temperatures of ordering in the magnetic subsystem and of the formation of a spiral

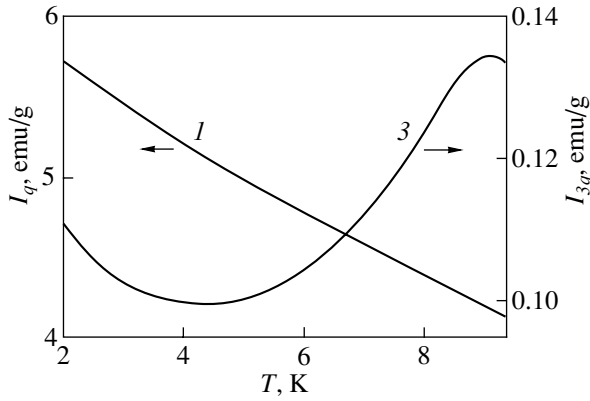


Fig. 5. Calculated temperature dependences of the intensities of (1) the fundamental (I_q) and (3) the third (I_{3q}) harmonics of the antiferromagnetism vector in copper metaborate at a zero applied field.

structure in it are different [and are given by Eqs. (11) and (12)] corresponds to the properties of copper metaborate described in Introduction. Indeed, for certain relations between the parameters of thermodynamic potential (5), we can obtain $T_p > T_{q2}$ and a stable homogeneous state ($\mathbf{q} = 0$) at intermediate temperatures. In this case, the temperature T_N for copper metaborate can be related to T_p given by Eq. (12) and T_i can be related to T_{q2} given by Eq. (11). Let us compare the relations derived for the temperature and field dependences of the wave vector and of the order parameters with the experimental data.

Figures 1–5 show the results of numerical calculation by Eqs. (6)–(16) using the following coefficients of the incomplete thermodynamic potential (5):

$$a_{11} = a_{22} = 3.3 \times 10^2 \frac{\text{G}^2 \text{g}^2}{\text{erg cm}^3 \text{K}},$$

$$T_1 = 0.19 \text{ K}, \quad T_2 = 20.4 \text{ K},$$

$$B_{22} = 5.2 \times 10^1 \frac{\text{G}^4 \text{g}^4}{\text{erg}^3 \text{cm}^3},$$

$$A_{12} = -1.8 \times 10^2 \frac{\text{G}^2 \text{g}^2}{\text{erg cm}^3},$$

$$C_{12} \left(\frac{2\pi}{c} \right) = -5.3 \times 10^3 \frac{\text{G}^2 \text{g}^2}{\text{erg cm}^3},$$

$$D_{11} \left(\frac{2\pi}{c} \right)^2 = 3.7 \times 10^4 \frac{\text{G}^2 \text{g}^2}{\text{erg cm}^3},$$

$$D_{22} = D_{11}, \quad D_{12} = 0.$$

As seen from Figs. 1–5, we failed to achieve excellent agreement between the calculated and experimental data; however, the calculated temperature and field

dependences of the parameters of the magnetic subsystem of copper metaborate are in satisfactory agreement with the experiment.

In the incommensurate phase, the spontaneous contribution to the magnetization of the whole crystal disappears because of the spiral structure and only the magnetization induced by an applied field is nonzero (Fig. 2) [1, 2]. As the applied field increases, a first-order transition to the easy-plane weak-ferromagnetic phase occurs; namely, the component of the antiferromagnetism vector with $\mathbf{q} \neq 0$ vanishes in a jump at the field $H_c(T)$, whereas the component with a zero wave vector increases in a jump [4, 5]. This behavior of the magnetic subsystem also manifests itself in the magnetization (Fig. 3), which is related to the antiferromagnetism vector through the Dzyaloshinskiĭ invariant (with coefficient A_{12}). The presence of this invariant corresponds to nonzero values of magnetization in a zero field when its field dependence is linearly approximated in fields above $H_c(T)$ [1, 2]. Figure 4 shows the experimental [2] and calculated temperature–field phase diagrams in the temperature range 4–10 K.

The presence of higher harmonics in the spiral of the incommensurate phase is characteristic of the temperature range where the Lifshitz invariant is comparable to the anisotropy invariant [9]. For magnetic systems described by a one-parameter thermodynamic potential, the wave vector \mathbf{q} differs from zero even at the ordering temperature ($T_i = T_p$) and the anisotropy invariant (which is proportional to $|\eta|^4$ for a tetragonal crystal) becomes comparable to the Lifshitz invariant (which is proportional to $q|\eta|^2$) substantially below T_i , near the transition to the low-temperature commensurate phase. In copper metaborate, however, q increases sharply from zero at $T_i < T_p$ (Fig. 1) [3] and the invariants can become comparable only in a narrow vicinity of T_i or in the range where q varies smoothly. According to the experimental data in [3], only the former possibility is realized.

Figure 5 shows the calculated temperature dependences of the intensities of the fundamental and third harmonics of the antiferromagnetism vector at a zero applied field. To describe them, we added the anisotropy invariant

$$\frac{E_{22}}{2} \int \eta_{21}^2 \eta_{22}^2 dV$$

to thermodynamic potential (5). The intensity of the fundamental harmonic is higher than that of the third harmonic by a factor of approximately 30 (as observed in [3] at $T = 9.35$ K) for $E_{22} = 7 (\text{G g})^4 / (\text{erg cm}^3)^3$. As seen from Fig. 5, this difference increases as the temperature decreases, which hampers the possible observation of the higher harmonic.

The sharp decrease in the intensity of magnetic peaks (3, 3, $\pm q$) at $T = 1.8$ K and the fact that thereafter q does not vary with decreasing temperature [4, 5] can be related to a lock-in transition to the commensurate

phase. This transition is accompanied by the sudden appearance of a gap in the energy spectrum of excitations that are transverse with respect to the order parameter and by the corresponding decrease in the correlation functions.

ACKNOWLEDGMENTS

We thank S.N. Martynov for helpful discussions.

This work was supported by the Ministry of Education of the Russian Federation (project no. E02-3.4-227) and the Russian Foundation for Basic Research (project no. 03-02-16701).

REFERENCES

1. G. Petrakovskii, D. Velikanov, A. Vorotinov, *et al.*, J. Magn. Magn. Mater. **205** (1), 105 (1999).
2. G. A. Petrakovskii, A. D. Balaev, and A. M. Vorotynov, Fiz. Tverd. Tela (St. Petersburg) **42** (2), 313 (2000) [Phys. Solid State **42**, 321 (2000)].
3. R. Roessli, J. Schefer, G. A. Petrakovskii, *et al.*, Phys. Rev. Lett. **86** (9), 1885 (2001).
4. J. Schefer, M. Boehm, B. Roessli, *et al.*, Appl. Phys. A **74** (Suppl. 1), S1740 (2002).
5. M. Boehm, B. Roessli, J. Schefer, *et al.*, Physica B (Amsterdam) **318** (4), 277 (2002).
6. Yu. A. Izyumov, *Neutron Diffraction by Long-Period Structures* (Énergoatomizdat, Moscow, 1987).
7. O. V. Kovalev, *Representations of the Crystallographic Space Groups: Irreducible Representations, Induced Representations, and Corepresentations* (Nauka, Moscow, 1986; Gordon and Breach, Yverdon, Switzerland, 1993).
8. L. D. Landau and E. M. Lifshitz, *Course of Theoretical Physics, Vol. 5: Statistical Physics*, 3rd ed. (Nauka, Moscow, 1976; Pergamon, Oxford, 1980), Part 1.
9. I. E. Dzyaloshinskii, Zh. Éksp. Teor. Fiz. **47** (3), 992 (1964) [Sov. Phys. JETP **20**, 573 (1964)].

Translated by K. Shakhlevich